Insulin Derived Fibrils Induce Cytotoxicity *in vitro* and Trigger Inflammation in Murine Models

Brianne E. Lewis, PhD[1], Adam Mulka, MS[1],
Li Mao, BS[1], Roshanak Sharafieh, PhD[2], Yi Qiao, MD[2],
Shereen Kesserwan, MS[1], Rong Wu, PhD[2], Don Kreutzer, PhD[2],
and Ulrike Klueh, PhD[1] (iD)

Abstract

Background: Effective exogenous insulin delivery is the cornerstone of insulin dependent diabetes mellitus management. Recent literature indicates that commercial insulin-induced tissue reaction and cellular cytotoxicity may contribute to variability in blood glucose as well as permanent loss of injection or infusion site architecture and function. It is well accepted that insulin formulations are susceptible to mechanical and chemical stresses that lead to insulin fibril formation. This study aims to characterize *in vitro* and *in vivo* toxicity, as well as pro-inflammatory activity of insulin fibrils.

Method: *In vitro* cell culture evaluated cytotoxicity and fibril uptake by macrophages and our modified murine air-pouch model quantified inflammatory activity. The latter employed FLOW cytometry and histopathology to characterize fibril-induced inflammation *in vivo*, which included fibril uptake by inflammatory phagocytes.

Results: These studies demonstrated that insulin derived fibrils are cytotoxic to cells *in vitro*. Furthermore, inflammation is induced in the murine air-pouch model *in vivo* and in response, macrophages uptake fibrils both *in vitro* and *in vivo*.

Conclusions: Administration of insulin fibrils can lead to cytotoxicity in macrophages. *In vivo* data demonstrate insulin fibrils to be pro-inflammatory which over time can lead to cumulative cell/tissue toxicity, inflammation, and destructive wound healing. Long term, these tissue reactions could contribute to loss of insulin injection site architecture and function.

Keywords
inflammation, insulin fibril, macrophage, subcutaneous insulin administration

Introduction

Currently, the American Diabetes Association estimates that 7.5 million Americans are insulin dependent and require frequent subcutaneous insulin administration (SIA) for glycemic control.[1] However, patients using multiple daily injections or continuous subcutaneous insulin infusion (CSII) can experience skin irritation, inflammation, and scarring at injection and CSII sites.[2-6] Thus, users are encouraged to rotate injection/CSII sites across multiple skin locations to minimize adverse events.[5,7,8] Even when following SIA best practices, several undesirable conditions can occur including hyperglycemia and diabetic ketoacidosis.[3,4,9] Given that diabetic complications are prevented when euglycemia is achieved, it is critical to understand mechanisms which contribute to unreliable insulin efficacy through the development of skin pathologies.[10-12]

There are several factors which may contribute to skin inflammation from injection or infusion pump therapy. Catheter material, direction of flow, injection or infused preservatives can all contribute to site inflammation.[13-16] In addition, insulin fibril formation can lead to adverse skin pathologies resulting in poor glycemic management.[17,18] The formation of insulin derived fibrils (IDF) have been well

[1]Department of Biomedical Engineering, Integrative Biosciences Center. Wayne State University, Detroit, MI, USA
[2]Department of Surgery, School of Medicine. University of Connecticut, Farmington, CT, USA

Corresponding Author:
Ulrike Klueh, PhD, Department of Biomedical Engineering, Integrative Biosciences Center, Wayne State University, 6135 Woodward Ave, Detroit, MI 48202, USA.
Email: klueh@wayne.edu

characterized biochemically and can form as a result of mechanical or chemical stressors.[1,19-22] In short, insulin fibrils are a large oligomer characterized by a non-native β-sheet structure rendering the protein inactive.[19,20] While biochemical fibril formation has been studied extensively *in vitro*, data for administration of fibrils *in vivo* is limited.[17,18] Thus, we hypothesize that insulin fibril formation represents another potential contributing factor for tissue reactions at sites of SIA or CSII and as such, it is critical to understand the impacts of fibril administration *in vivo.*[2]

In this report, we utilized streptozotocin (STZ) induced diabetic mice to evaluate tissue response in a modified air pouch which allows for the collection of tissue, cell and fluid contents at injection sites.[15,16] Furthermore, the air pouch provides a defined, subcutaneous space for evaluation of injection reagents. Our *in vitro* studies use murine cell lines found in the subcutaneous area to evaluate cytotoxicity of insulin fibrils and to elucidate a mechanism for fibril uptake. Results are compared to the inflammatory and cytotoxicity of phenolic preservatives (PP) found in insulin formulations as a previously established inflammatory agent.[15,16,23] The goal of the present study is to examine the relative contributions to tissue inflammation during repeated SIA with respect to the variables of insulin derived fibrils (IDF) and insulin phenolic preservatives (PP).

Methods

Cell types: Mouse cell lines include macrophages (RAW 264.7) and embryonic fibroblasts (3T3-L1), which were purchased from ATCC bio products (Manassas, VA) and cultured following the supplier's protocol. 3T3 Fat cells were induced from 3T3-L1 using MDI cocktail (methylisobutylxanthine, dexamethasone and insulin).[24]

Insulin fibril generation: Fibril species were generated by incubating Humalog® at 37°C and 300 rpm in a sterile polystyrene culture tube for 24 hours. Following incubation, fibril species were centrifuged and washed 3 times with sterile saline. Subsequently, they were resuspended and diluted in either saline (denoted saline fibril) or diluent (denoted diluent fibril) at a ratio of 1:2. Diluent is commercially available from Eli Lilly and is utilized as a source of pharmaceutical grade phenolic preservative.[15] Diluent and diluent fibrils have a combined PP concentration of 2.25 mg/ml (1.6 mg/ml m-cresol, 0.65 mg/mL phenol). As a comparison, saline fibrils contain no PP.

Insulin derived fibril (IDF) uptake studies using murine macrophages in vitro: Initially, thioglycolate induced macrophages (MQ) were obtained from MaFIA (Macrophage Fas-Induced Apoptosis) or normal C57BL/6 mice, cultured in vitro in RPMI 1640 and 10% fetal calf serum at 37°C and 5% CO_2, and validated using anti-F4/80 antibody/immunohistochemistry, and nucleus morphology to confirm the resulting cells identity as MQs.[25] These MQs were cultured with the various dilutions of the non-florescent or Alexa Fluor 594 containing IDF stock solutions (1/10, 1/30 and 1/90) for

24 hours at 37°C and 5% CO_2. The cultures were then washed with RPMI 1640 media 3 times, before analysis as described. Both C57BL/6 and MaFIA mice were obtained from Jackson Laboratory (Bar Harbor, Maine). The MaFIA mice express Enhanced Green Fluorescent Protein (EGFP) in 78% of isolated peritoneal macrophages.[26]

MTT cytotoxicity assay: Murine cells were plated in a 48-well plate with 2.5×10^5 cells/well in 250 μl of media (DMEM) without phenol red containing 10% fetal bovine serum and 1% penicillin/streptomycin. Following an overnight incubation, cells were treated with test agents from 1:3 to 1:192 then reincubated at 37°C for 3 days. An MTT assay (ATCC bio products Manassas, VA) was performed according to the manufacturer's protocol as described previously.[15]

Mice: Hsd:ICR(CD-1) mice were purchased from Envigo (Somerset, NJ) or bred in-house. Mice were maintained under temperature- and light-controlled conditions (20-24°C, 12-h light-dark cycle) receiving food and water ad libitum. Mice utilized in these studies had an average weight between 30-40 g, 8-10 weeks and were test naïve. A power analysis was performed in order to determine the total number of mice in these studies required to have an 80% chance of detecting a statistically significant difference between these groups at a 95% confidence interval. Each treatment group consisted of 6-9 mice. All studies were conducted with approval from the institutional animal care and use committee (IACUC) at Wayne State University.

Streptozotocin induced diabetes in mice: Diabetes was induced following the protocol developed by Furman.[27] Male mice received a daily intraperitoneal (i.p.) injection of streptozotocin (STZ) (50 mg STZ/kg body weight) for a period of 5 days (Sigma-Aldrich, St. Louis, MO). Blood glucose levels were monitored at least twice weekly following STZ treatment using a Bayer Contour Next EZ Meter (Ascensia Diabetes Care, Parsippany, NJ). Mice with a blood glucose level above 250 mg/dL on 2 sequential blood glucose samples were designated as diabetic.

Murine Air Pouch Model of Tissue Toxicity and inflammation: The classic murine air pouch model was adapted to evaluate the tissue response to injected agents as previously described.[15] Test agents for all studies were injected once daily, (3 days after air pouch initiation), with a volume of 300 μL of saline, diluent (Eli Lilly), saline fibril or diluent fibril into the air pouch. Volume of 300 uL was chosen to effectively cover the surface area of the air pouch to elicit a tissue response, which correlates to injected 0.5 mg insulin equivalents of fibrils. It should be noted that IDF have no effect on blood glucose levels and can be used in both normal and diabetic mice without a hypoglycemic risk. Contents of the air pouch were analyzed using total cell number counts, flow cytometry analysis, and through standard histopathological analysis. Analyses were performed at 3 and 7 days. The initial time point was chosen to reflect FDA approved lifespan for insulin infusion and injection devices whereas 7 days was chosen as an end-stage time point that was more than twice the approved lifespan.[2,4]

Leukocyte isolation from mouse air pouch and fluorescence-activated cell sorting (FACS): After 3 or 7-days of treatment, mice were euthanized (CO_2 inhalation and cervical dislocation) and the air pouch was lavaged with a total of 10 mL of 0.9% saline (Baxter, Deerfield, IL). The collected cell fluid was processed as previously described.[15] The total leukocyte population was then subjected to flow cytometry analysis (FACS) using fluorescent labeled antibodies (1:100) (BioLegend, SanDiego, CA) to detect myeloid cells ($CD45^+CD11b^+$), neutrophils ($CD45^+CD11b^+Ly6G^+$), macrophages ($CD45^+$ $CD11b^+$ $Ly6G^-$ $Ly6G^{low}$), monocytes ($CD45^+$ $CD11b^+$ $Ly6G^-$ $Ly6G^{high}$), and lymphocytes (SSC-A^- $CD45^{high}$).[24] Fluorescent minus one (FMO) controls were used to differentiate between positively and negatively stained populations. Compensation was performed using BD Comp Beads (BD Biosciences, San Jose, CA) to create single-color controls of each antibody. FACS analyses were performed on a BD-LSRII utilizing the services of the microscopy, imaging, and cytometry core laboratory (MICR), at Wayne State University, Detroit, MI, and the data were analyzed with FlowJo software (FlowJo, LLC).

Statistical analysis: All analyses were conducted using SAS VERSION 9.4 (SAS, INC., Cary, NC). For normative data comparing 2 groups, a 2-tailed t-test was employed to detect a significant difference at a 95% confidence interval. For multiple group comparisons, a one-way ANOVA test was performed to assess for statistical significance at a 95% confidence interval. If significance was detected, then a post-hoc Tukey test was utilized to assess for statistically significant differences among the subgroups assessed in the ANOVA test. Following FACS staining and analysis of the cell populations, all cell numbers were graphed in a boxplot using GraphPad Prism 8 software.

Histopathologic evaluation: Histological evaluation was followed as previously described by our laboratory.[15] To evaluate tissue responses to the daily air pouch injections, qualitative histopathologic evaluation was performed on mouse tissue samples at 3- and 7-days post-injection. Tissue samples were fixed in 10% buffered formalin (VWR, Radnor, PA) for 24 hours followed by standard tissue preparatory steps, paraffin embedding, and sectioning. Tissue samples were cut into 5 μm sections and stained using Hematoxylin and Eosin stain (H&E). To confirm the presence of macrophages in the air pouch, tissue sections were stained with a mouse macrophage-specific antibody designated anti-mouse F4/80 (Fisher Scientific, catalog # MF48000). Mouse IgG was used as a negative control. Anti-insulin antibody (Invitrogen, PA1-26938) was incubated at 1:100 followed by IgG-HRP conjugate antibody (Invitrogen, A18769) at 1:500. Tissue samples were evaluated using a Nikon microscope and imaging system.

Results

Cellular cytotoxicity of insulin fibrils *in vitro*. Cellular cytotoxicity *in vitro* for saline, diluent and insulin, saline
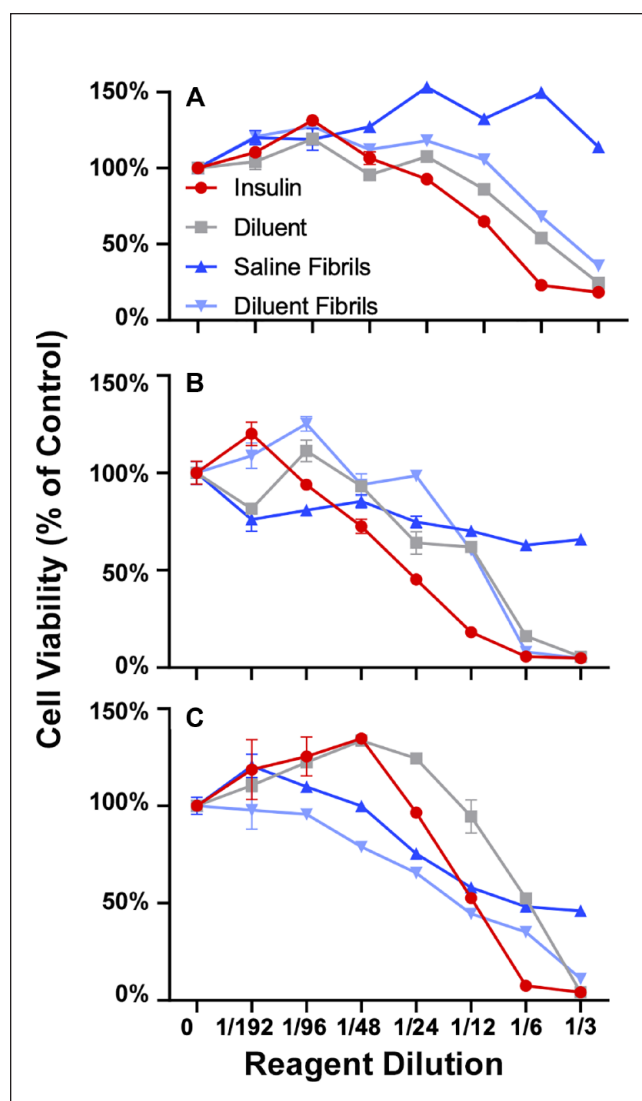

Figure 1. Determination of cellular cytotoxicity of phenolic preservatives and insulin fibrils in murine cell lines and primary cultures in vitro. To determine the in vitro cytotoxicity of phenolic compounds and insulin fibrils in murine cell lines, as well as primary cultures in vitro MTT cytotoxicity assays were used after 3 days of co-culture of cells and test agents. MTT assay was used for 3T3-L1 fibroblast cells (A), 3T3-Fat induced cells (B), raw macrophage (C), following 3-day in vitro incubation with agents. Each panel shows cells treated with diluent (grey) diluent + fibril (light blue), saline + fibril (dark blue), or insulin (red) at increasing concentrations. Cell viability is expressed as percent to saline control. MTT assay (panels A-C) data reflect absorbance at 570 nm. Error bars represent standard deviation. The concentration of all test reagents is based on dilutions in media. Full statistical analysis is presented in supplemental section Table S1.

fibrils or diluent fibrils at increasing concentrations (Figure 1) was determined using the MTT assay. Diluent, insulin and diluent fibril all contain PP.[15] Cytotoxicity was not observed for saline treatment for any mouse cell line. Any treatment containing phenolic preservatives, (eg, insulin, diluent and
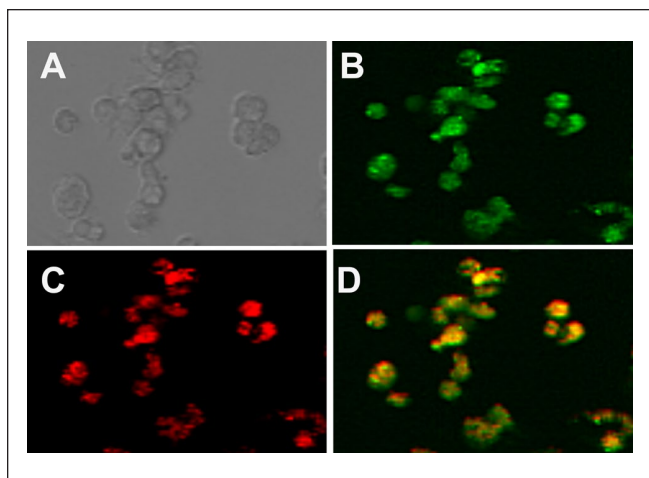
Figure 2. Immunofluorescence of fibril uptake in isolated macrophages. Bright field microscopy of isolated macrophages is shown in (A). MaFIA isolated macrophages expressing GFP (B) and IDF conjugated to alexafluor 594 (C). Overlay of GFP and alexafluor 594 results in yellow after 24 hours of macrophage incubation with IDF (D).

diluent fibril), was cytotoxic for all cell types at 1:12 dilution or higher irrespective of fibril addition. Saline fibril had a cytotoxic effect for murine macrophage cell lines but not for any other cell line. Specifically, cytotoxicity for diluent fibril paralleled saline fibril for murine macrophages indicative of a toxic effect of fibril for this cell line. This study underscores the finding that fibril cytotoxicity is highly cell type dependent.

Insulin-derived fibril uptake by murine macrophages *in vitro.* As a result of the in vitro cytotoxicity studies, we hypothesized that IDF uptake (phagocytosis) triggered macrophage (MQ) toxicity. This was evaluated using Alexa Fluor 594 conjugated to IDF against GFP expressing MQ cells. We demonstrated that IDF were phagocytized by murine MQs in vitro (Figure 2). MaFIA GFP-MQ (Figure 2B) readily phagocytosed IDF-Alexa Fluor 594 (Figure 2C). Merging of the fluorescent images resulted in bright yellow particles of IDF associated with the green MQ (Figure 2D).

Analysis of lavage fluids following injection of test agents. The tissue toxicity of phenolic preservatives and fibril was determined by daily injection of saline (S), diluent (D), saline fibril (SF) or diluent fibril (DF) into the mouse air pouch of non-diabetic and diabetic mice for either 3 days (3D) or 7 days (7D). No adverse events were recorded during agent administration and animals were healthy prior to start of experiment. Total cell recruitment in response to test agents is shown in Figure 3A with subpopulations depicted in Figure 3B and D. Statistical analysis of cell counts and raw data are found in supplementary data. Total cell recruitment statistical analysis demonstrated significance ($P < .05$) for all test agents with the exception of saline vs diluent in non-diabetic (3-days) and diabetic

mice (7-days). Significance was not observed for test agents when comparing duration of treatment for 3 and 7 days except for diluent in non-diabetic mice and saline in diabetic mice. Diabetic state compared to non-diabetic state however resulted in increased total cell recruitment for all test agents (S, D, SF, DF) at each time point where $P < .01$ for all. Next, increased neutrophil recruitment was observed for diluent vs diluent fibril treatments ($P < .05$) except for diabetic 3-day injections. Saline vs saline fibril was significant for 7-day non-diabetic and 3-day diabetic groups only. Again, duration of treatment (3 days vs 7 days) when comparing test agents for both non-diabetic and diabetic mice was not significant except for saline fibril in non-diabetic mice, diluent and diluent fibril in diabetic mice. Neutrophil recruitment was not significant for all saline versus diluent groups. Overall neutrophil recruitment did not display a clear trend across treatment groups and future work is needed to elucidate their role in SIA. However, this is in contrast to macrophage cell recruitment where all fibril treatments are significant compared to their control (S vs SF; D vs DF). The diabetic state also demonstrates enhanced macrophage recruitment compared to non-diabetic mice for all treatment groups ($P < .05$ for all) whereas the duration of treatment had little effect. Finally, lymphocyte recruitment was enhanced for diluent vs diluent fibril groups and saline fibril vs diluent fibril groups ($P < .05$) with the exception of 7 day and 3-day diabetic respectively.

Histopathologic tissue analysis following 3- and 7-days injections of test agents for non-diabetic mice: Tissue response was evaluated through standard histopathology following air pouch lavage after injection of test agents for 3-days (Figure 4) and 7-days (Figure 5). Histopathological evaluation revealed that both saline (Figure 4A, I and Q) and diluent (Figure 4B, J and R) injection into the air pouch displayed light scattering of inflammatory cells with a more intense gathering of inflammatory cells at the air pouch tissue interface (Figure 4). Most of the sparse accumulations of inflammatory cells were predominately neutrophils and macrophages as confirmed using F4/80 immunohistochemistry. Polymorphonuclear leukocytes (PMN), which are F4/80 negative, were also detected morphologically by H&E analysis. Analysis of macrophage distribution demonstrated limited numbers of macrophages present for both saline (Figures 4E, M and U) and diluent (Figure 4F, N and V) injections. Saline fibril (Figures 4C, K and S) and diluent fibril injection (Figure 4D, L and T) displayed neutrophils and macrophages present at the air pouch interface whereas macrophages were the predominant cell in these 2 treatment groups with a higher count in the diluent fibril treatment group (Figure 4H, P and X). Overall, the tissue reactions after 7-days (Figure 5) were comparable to the saline and diluent injection over the 3-day injection period (Figure 4). However, saline fibril injection (Figure 5C, K and S) over the 7-day period demonstrated slightly more inflammatory cell presence when compared to saline or diluent injection over the 3-day period.
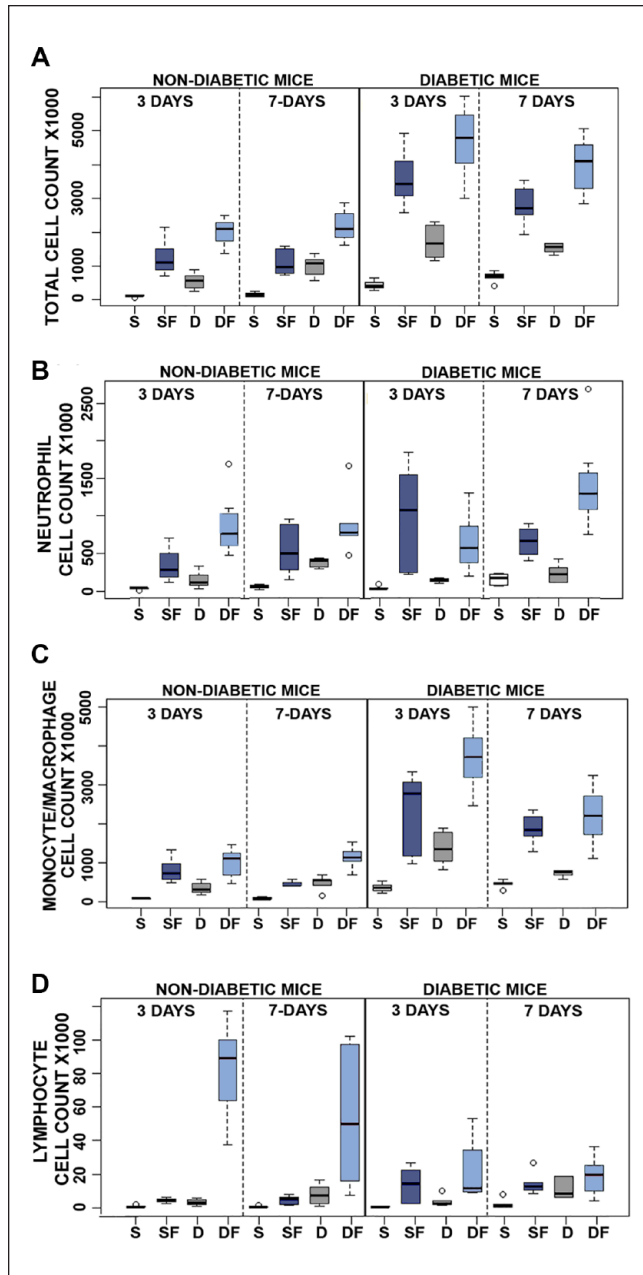
Figure 3. Quantitative analysis of pro-inflammatory reactivity of insulin fibrils and phenolic compounds *in vivo* using the murine air pouch (MAP) model in non-diabetic and diabetic mice: evaluation of 3 and 7 days of treatment. Results of flow analysis show total cell recruitment (A) and cell type subpopulation for neutrophils (B), monocytes/macrophages (C), and lymphocytes (D), for each treatment: saline (S), diluent (D), saline + fibril (SF) or diluent + fibril (DF). All results are expressed as total cell count ×1000, and were obtained by flow cytometry (*N* = 6–9). Open circles denote outliers. Statistical analysis of this data is presented in Tables S2–5.

Diluent fibril injection showed enhanced presence of inflammatory cells including enhanced cellularity at the air pouch interface (Figure 5D, L and T). Further analysis indicated that macrophages were substantially more present in the

fibril injected air pouch regardless of saline (Figure 5G, O and W) or diluent (Figure 5H, P and X) suspension.

Histopathologic tissue analysis following 3- and 7-days injections of S, D, SF, DF for diabetic mice. In general, all tissue reactions, except the saline treatment group, were substantially increased in the chemically-induced diabetic animals. For 3-day treatment of diluent-injections, (Figure 4BB, JJ, and RR) air pouch showed slight scattering of neutrophils and macrophages lining the air pouch wall. Sparse numbers of macrophages present in the tissue adjacent to the air pouch as evident in F4/80 macrophage specific stain (Figures 4FF, NN, and VV). In comparison, the 7-day injections of diluent tissue displayed a notable accumulation of MQ at the air-tissue interface (Figure 5BB, JJ and RR). Tissue treatment with saline fibril for 3-days (Figures 4CC, KK, and SS) and diluent fibril for 3-days (Figures 4DD, LL, and TT) injection is interesting in such that a similar accumulation of inflammatory cells surrounds the air pouch tissue for both treatment groups. MQ were spread throughout the air pouch tissue, and frequently appeared larger and had substantial presence of proteinaceous material in their cytoplasm (e.g. red staining material in H&E-stained slides) (Figure 3DD, LL and TT). These results were also observed in the 7-day injection treatment with saline (Figure 5CC, KK and SS) and diluent fibrils (Figure 5DD, LL and TT) where substantial amounts of inflammatory cells are present. Further analysis with macrophage specific stain F4/80 indicated macrophage presence for both 7-day injection of saline fibril (Figure 5GG, OO and WW) and 7-day injection of diluent fibril (Figure 5HH, PP and XX). The qualitative nature of histopathology makes it difficult to distinguish differences between the 3- and 7-day treatment groups. However, when comparing the histopathologic evaluation of the air pouch tissue, a stronger reaction is observed in the fibril-injected air pouch, irrespective of saline or diluent suspension, indicating that the fibril itself contributes to the tissue reaction.

Insulin-derived fibril distribution in air pouch tissue. Following fibril injection, irrespective of suspension in saline or diluent agent, a notable appearance of amorphous pink staining material, both within and outside of PMN and MQ was observed (Figure 6). MQ appeared larger with enhanced presence of cytoplasmic proteinaceous material. Anti-insulin staining determined that this amorphous proteinaceous intracellular and extracellular material consisted of insulin fibrils for non-diabetic mice over the period of 3-days (Figure 6A and B) and 7-days (Figures 6E and F). No difference in anti-insulin staining was observed for chemically induced diabetic mice over the same 2 time periods (Figure 6I, J, M and N). Normal IgG did not experience any specific or non-specific insulin staining for all treatment conditions irrespective of non-diabetic or diabetic mic (Figure 6C, D, G–P). Of note is that anti-insulin antibodies used in these studies detect both human and mouse insulin and insulin fibrils. However, anti-insulin immuno-histochemical analysis of the air pouch tissue indicated that no human or
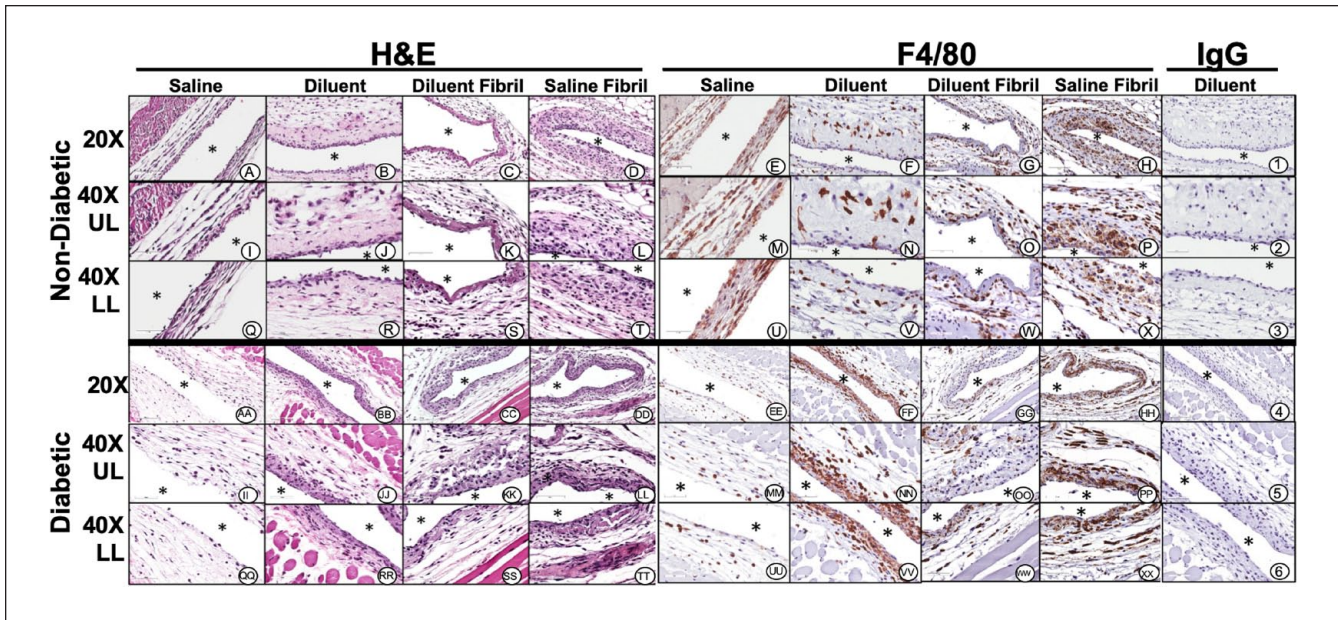
Figure 4. Histopathologic and immunohistochemical evaluation of mouse air-pouch tissue (post lavage) from non-diabetic and diabetic mice after 3 days treatment with insulin fibrils and phenolic diluent. Representative photo-micrographs of tissue reactions from 3-day treated non-diabetic and diabetic mice (post lavage) including: saline, diluent, saline fibril and diluent fibril treated non-diabetic and diabetic mice. Matched tissue sections were stained for general histopathology using H&E staining, and for macrophages using Anti-F4/40 antibody or matched non-immune IgG. All photo-micrographs were taken at 20× or 40× as designated. Each area of the MAP tissue evaluated in the study is designated as: UL (upper layer of MAP tissue), and LL (lower level MAP tissue), respectively. White area containing (*) indicates air space location of murine air pouch.
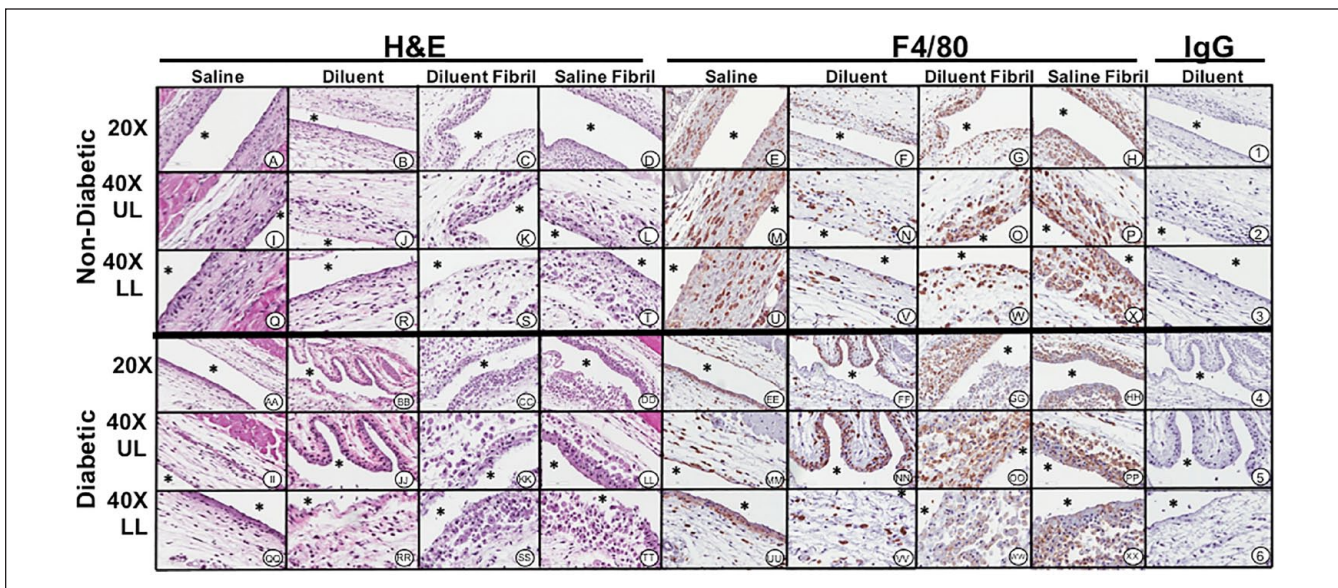

Figure 5. Histopathologic and immunohistochemical evaluation of mouse air-pouch tissue (post lavage) from non-diabetic and diabetic mice after 7 days treatment with insulin fibrils and phenolic diluent. Representative photo-micrographs of tissue reactions from 7-day treated non-diabetic and diabetic mice (post lavage) including: saline, diluent, saline fibril and diluent fibril treated non-diabetic and diabetic mice. Matched tissue sections were stained for general histopathology using H&E staining, and for macrophages using Anti-F4/40 antibody or matched non-immune IgG. All photo-micrographs were taken at 20× or 40× as designated. Each area of the MAP tissue evaluated in the study is designated as: UL (upper layer of MAP tissue), and LL (lower level MAP tissue), respectively. White area containing (*) indicates air space location of murine air pouch.
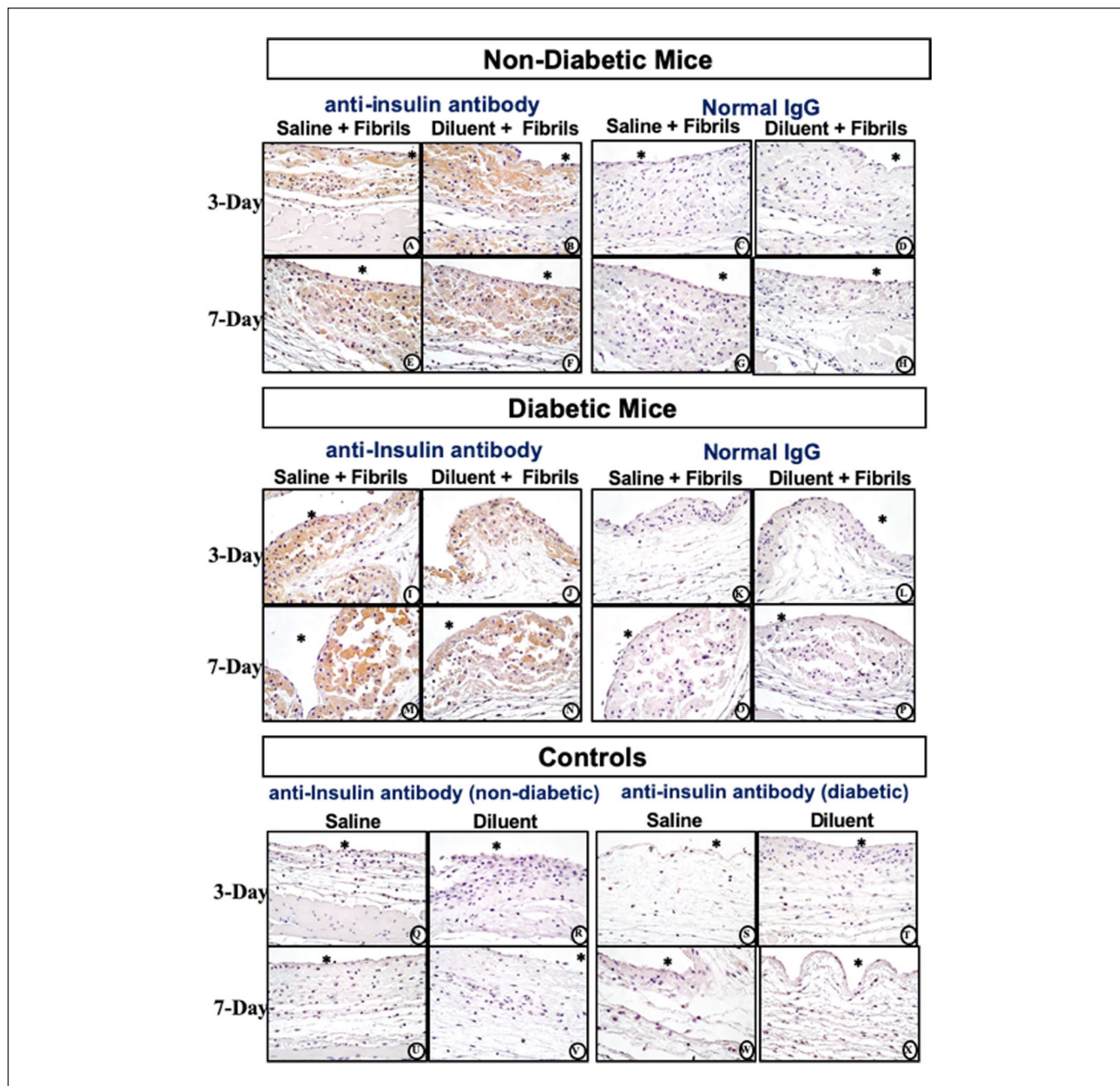
Figure 6. Histopathologic and Immunohistochemical evaluation of mouse air-pouch tissue (post lavage) from non-diabetic and diabetic mice after 3-and 7-days treatment with insulin fibrils. Matched tissue sections were stained for anti-insulin or non-immune IgG. Representative photo-micrographs of tissue reactions from 3 and 7 day treated with insulin fibrils for non-diabetic mice (top) and diabetic mice (middle). Background controls for anti-insulin stain for non-diabetic and diabetic mice treated with saline and diluent are shown in bottom panel. All photo-micrographs were taken at 40×. White area containing (*) indicates air space location of the murine air pouch.

mouse insulin or insulin fibrils were detectable in control air pouch tissues treated with saline or diluent (Figure 6Q–X).

Discussion

These data indicate that insulin derived fibrils contribute to tissue inflammation during SIA. Our study assessed both *in vitro* cell culture studies and a mouse air-pouch model

designed to analyze cellular and tissue reactions following repeated injections with saline, PP, diluent, and fibrils suspended in either saline or diluent. The *in vitro* studies investigating cytotoxicity of PP and insulin fibrils suspended in saline or diluent demonstrated a macrophage specific cytotoxicity for the fibril addition (Figure 1). Mouse fibroblast and fat cells exhibited cytotoxicity towards the PP diluent, to insulin and to diluent fibril but not to saline fibril. This

indicates that PP is cytotoxic to these cell lines whereas, the MQ cell line demonstrated cytotoxicity towards PP as well as fibrils. This suggests that fibril cytotoxicity is highly dependent on the cell type. Future studies should elucidate MQ death mechanisms following fibril phagocytosis.

Our *in vivo* data supplemented the *in vitro* findings. Specifically, FACS data revealed that MQ are recruited *in vivo* to the injection site when treated with diluent or saline fibril species (Figure 3). Total cell recruitment supports the hypothesis that fibril species and PP-containing diluent are pro-inflammatory. Influx of inflammatory cells is increased in the presence of insulin-derived fibril. Notably, saline versus diluent did not show any significant differences in inflammatory cell numbers for either 3-day in non-diabetic or 7-day in diabetic CD-1 mice, which is in contrast to our previously published results investigating infusion of these agents.[15] We attribute these differences to the different amounts of fluids administered between these 2 studies and duration of exposure. In the published infusion studies,[15] a total of 1.2 mL/day were administered continuously whereas the current study utilized a total of 0.3 mL once per day, suggesting a toxicity threshold of the diluent.

Histopathological evaluations of the air pouch tissue post lavage demonstrated that saline fibril and diluent fibril are equally capable of inducing inflammation characterized by an influx of PMNs and monocytes/macrophages (Figures 4 and 5). Notably the concentration of fibril solution injected into the air pouch is unlikely to be encountered clinically. Future follow-up studies should be designed to characterize a dose-response curve. Notwithstanding, it is likely that even small amounts of fibril could induce severe IDF that would alter tissue architecture and function rendering this injection or infusion site unusable. Irrespective of the saline or diluent agent utilized for fibril injections, the post lavage air pouch tissue site demonstrated neutrophils and macrophages phagocytizing insulin fibrils. An amorphous pink staining material was observed both external and internal to the PMN and MQ (Figures 4 and 5). The impact of fibril uptake by phagocytes on cell function and proinflammatory activity including the expression of proinflammatory cytokines will need to be investigated to determine the mediators and mechanisms of fibril-induced inflammation. Moreover, the potential contribution exhibited by ongoing leukocyte mediated fibril uptake and possible cell necrosis needs investigation. As diabetes is a chronic illness, one of the cornerstones of diabetic management is to maximize the availability of useful injection or infusion sites. Any strategy designed to optimize exogenous insulin administration and efficacy must mitigate pro-inflammatory factors including IDF.

Conclusions

Administration of insulin fibrils can lead to cytotoxicity, specifically in macrophages. *In vivo* data demonstrate insulin fibrils to be pro-inflammatory which over time can lead to cumulative cell/tissue toxicity, inflammation, and destructive wound healing. Long term, these tissue reactions could contribute to loss of insulin injection site architecture and function.

Abbreviations

CSII, continuous subcutaneous insulin infusion; FACS, fluorescence-activated cell sorting; IDF, insulin derived fibril; MQ, macrophage; PMN, polymorphonuclear leukocytes; PP, phenolic preservatives; SIA, subcutaneous insulin administration; STZ, streptozotocin.

Declaration of Conflicting Interests

The author(s) declared the following potential conflicts of interest with respect to the research, authorship, and/or publication of this article: Ulrike Klueh, PhD and Don Kreutzer, PhD are co-founders and co- owners of the small business Cell and Molecular Tissue Engineering, LLC, Avon CT. No other potential conflicts of interest relevant to this article are present.

ORCID iD

Ulrike Klueh https://orcid.org/0000-0003-1104-7704

Supplemental Material

Supplemental material for this article is available online.

References

1. Cefalu WT, Dawes DE, Gavlak G, et al. Insulin access and affordability working group: conclusions and recommendations. *Diabetes Care*. 2018;41(6):1299-1311. doi:10.2337/dci18-0019
2. Simic A, Schøndorff PK, Stumpe T, et al. Survival assessment of the extended-wear insulin infusion set featuring lantern technology in adults with type 1 diabetes by the glucose clamp technique. *Diabetes Obes Metab*. 2021;23(6):1402-1408. doi:doi:10.1111/dom.14337

3. Evert AB, Bode BW, Buckingham BA, et al. Improving patient experience with insulin infusion sets: practical guidelines and future directions. *Diabetes Educ*. 2016;42(4):470-84. doi:10.1177/0145721716642526

4. Schmid V, Hohberg C, Borchert M, Forst T, Pfützner A. Pilot study for assessment of optimal frequency for changing catheters in insulin pump therapy-trouble starts on day 3. *J Diabetes Sci Technol*. 2010;4(4):976-982. doi:10.1177/193229681000400429

5. Al Hayek AA, Robert AA, Al Dawish MA. Skin-related complications among adolescents with type 1 diabetes using insulin pump therapy. *Clin Med Insights Endocrinol Diabetes*. 2018;11:1179551418798794. doi:10.1177/1179551418798794

6. Berg AK, Thorsen SU, Thyssen JP, Zachariae C, Keiding H, Svensson J. Cost of treating skin problems in patients with diabetes who use insulin pumps and/or glucose sensors. *Diabetes Technol Ther*. 2020;9(1557-8593):658-665. doi:10.1089/dia.2019.0368

7. Patton SR, Eder S, Schwab J, Sisson CM. Survey of insulin site rotation in youth with type 1 diabetes mellitus. *J Pediatr Health Care*. 2010;24(6):365-371. doi:10.1016/j.pedhc.2009.11.002

8. Zhang JY, Shang T, Chattaraj S, et al. Advances in insulin pump infusion sets symposium report. *J Diabetes Sci Technol*. 2021;15(3):705-709. doi:10.1177/1932296821999080

9. Swan KL, Dziura JD, Steil GM, et al. Effect of age of infusion site and type of rapid-acting analog on pharmacodynamic parameters of insulin boluses in youth with type 1 diabetes receiving insulin pump therapy. *Diabetes Care*. 2009;32(2):240-244. doi:10.2337/dc08-0595

10. Foster NC, Beck RW, Miller KM, et al. State of type 1 diabetes management and outcomes from the T1D exchange in 2016-2018. *Diabetes Technol Ther*. 2019;21(2):66-72. doi:10.1089/dia.2018.0384

11. Aschner P, Horton E, Leiter LA, Munro N, Skyler JS; Global Partnership for Effective Diabetes Management. Practical steps to improving the management of type 1 diabetes: recommendations from the Global Partnership for Effective Diabetes Management. *Int J Clin Pract*. 2010;64(3):305-315. doi:10.1111/j.1742-1241.2009.02296.x

12. Karges B, Schwandt A, Heidtmann B, et al. Association of insulin pump therapy vs insulin injection therapy with severe hypoglycemia, ketoacidosis, and glycemic control among children, adolescents, and young adults with type 1 diabetes. *JAMA*. 2017;318(14):1358-1366. doi:10.1001/jama.2017.13994

13. Hauzenberger JR, Hipszer BR, Loeum C, et al. Detailed analysis of insulin absorption variability and the tissue response to continuous subcutaneous insulin infusion catheter implantation in swine. *Diabetes Technol Ther*. 2017;19(11):641-650. doi:10.1089/dia.2017.0175

14. Hauzenberger JR, Münzker J, Kotzbeck P, et al. Systematic in vivo evaluation of the time-dependent inflammatory response to steel and Teflon insulin infusion catheters. *Sci Rep*. 2018;8(1):1132. doi:10.1038/s41598-017-18790-0

15. Kesserwan S, Mulka A, Sharafieh R, et al. Advancing continuous subcutaneous insulin infusion in vivo: new insights into tissue challenges. *J Biomed Mater Res A*. 2021; 109(7):1065-1079. doi:10.1002/jbm.a.37097

16. Mulka A, Lewis BE, Mao L, et al. Phenolic preservative removal from commercial insulin formulations reduces tissue inflammation while maintaining euglycemia. *ACS Pharmacol Transl Sci*. 2021;4(3):1161-1174. doi:10.1021/acsptsci.1c00047

17. Nakamura M, Misumi Y, Nomura T, et al. Extreme adhesion activity of amyloid fibrils induces subcutaneous insulin resistance. *Diabetes*. 2019;68(3):609. doi:10.2337/db18-0846

18. Iwaya K, Zako T, Fukunaga J, et al. Toxicity of insulin-derived amyloidosis: a case report. *BMC Endocr Disord*. 2019;19(1):61. doi:10.1186/s12902-019-0385-0

19. Choi JH, May BCH, Wille H, Cohen FE. Molecular modeling of the misfolded insulin subunit and amyloid fibril. *Biophys J*. 2009;97(12):3187-3195. doi:10.1016/j.bpj.2009.09.042

20. Ivanova MI, Sievers SA, Sawaya MR, Wall JS, Eisenberg D. Molecular basis for insulin fibril assembly. *Proc Natl Acad Sci USA*. 2009;106(45):18990-18995. doi:10.1073/pnas.0910080106

21. Rambaran RN, Serpell LC. Amyloid fibrils: abnormal protein assembly. *Prion*. 2008;2(3):112-117. doi:10.4161/pri.2.3.7488

22. Woods RJ, Alarcón J, McVey E, Pettis RJ. Intrinsic fibrillation of fast-acting insulin analogs. *J Diabetes Sci Technol*. 2012;6(2):265-276. doi:10.1177/193229681200600209

23. Weber C, Kammerer D, Streit B, Licht AH. Phenolic excipients of insulin formulations induce cell death, pro-inflammatory signaling and MCP-1 release. *Toxicol Rep*. 2014;2:194-202. doi:10.1016/j.toxrep.2014.11.019

24. Madsen L, Petersen RK, Sørensen MB, et al. Adipocyte differentiation of 3T3-L1 preadipocytes is dependent on lipoxygenase activity during the initial stages of the differentiation process. *Biochem J*. 2003;375(Pt 3):539-549. doi:10.1042/bj20030503

25. Klueh U, Frailey JT, Qiao Y, Antar O, Kreutzer DL. Cell based metabolic barriers to glucose diffusion: macrophages and continuous glucose monitoring. *Biomaterials*. 2014;35(10):3145-3153. doi:10.1016/j.biomaterials.2014.01.001

26. Burnett SH, Kershen EJ, Zhang J, et al. Conditional macrophage ablation in transgenic mice expressing a Fas-based suicide gene. *J Leukoc Biol*. 2004;75(4):612-623. doi:10.1189/jlb.0903442

27. Furman BL. Streptozotocin-induced diabetic models in mice and rats. *Curr Protoc Pharmacol*. 2015;70:5.47.1-5.47.20. doi:10.1002/0471141755